12
7-11-91 JS ①

UCRL-ID-104729

Thermocouple Psychrometer Measurements of In Situ Water Potential Changes in Heated Welded Tuff

Nai-hsien Mao
and
Herbert F. Wang

Manuscript Date: September 1990
Publication Date: May 1991

Lawrence Livermore National Laboratory

Work performed under the auspices of the U.S. Department of Energy by the Lawrence Livermore National Laboratory under Contract W-7405-Eng-48.

UCRL-ID--104729

DE91 015087

Thermocouple Psychrometer Measurements of In Situ Water Potential Changes in Heated Welded Tuff

Nai-hsien Mao and Herbert F. Wang

Abstract

Ten thermocouple psychrometers (TCPs) to measure water potential (WP) were installed in three holes in G-Tunnel at the Nevada Test Site as part of the Prototype Engineered Barrier System Field Tests. These integrated tests measured several parameters as a function of location and time within a few meters of a heater emplaced in welded tuff. The primary goal of the TCP experiment was to find out whether the combination of laboratory calibration and field use of the TCP can provide useful data for determining the change of moisture condition in the field. We calibrated the TCPs in NaCl solutions up to 80°C (176°F) in the laboratory. In two holes, we used rubber sleeves and packers to house TCPs, and in the third hole, we used foam. All three holes were grouted behind the TCP assemblages. Field results of the heater test showed that small temperature gradients were present for all measurements. Nevertheless, the WP calibration made the necessary correction for the nonisothermal condition. The initial moisture condition indicated by TCP data was about 99.5% relative humidity or a WP of about –5 bar. This corresponded to 15.4 g/m^3 of water in the air near the borehole wall, which was much wetter than we expected. A drying and re-wetting cycle peaked at about day 140 with a WP of –65 bar in borehole P3, located below the heater. A similar cycle but reduced in scale was found at about day 175 with a WP of –45 bar in borehole P2, above the heater. This difference in drying behavior above and below the heater was also observed from neutron data and was explained as a gravity effect. As temperatures increased, the evaporation rate of pore water increased. In unfractured rock, the gas-phase flow was primarily outward. Water condensed above the heater would drain back to keep the boiling region wet, but water condensed below the heater would drain away from the boiling region. This conceptual model explained both the time and magnitude differences for data from holes above and below the heater.

Introduction

The primary goal of the thermocouple psychrometer (TCP) experiment was to find out whether the combination of laboratory calibration and field use of the TCP can provide useful data for determining the change of moisture condition in the field. The water potential (WP) in the near field of the waste package is an important hydrologic parameter. Water potential is a function of relative humidity (Lang, 1967):

$$\mathrm{WP} = (1000RT/W_{\mathrm{A}})\ln(p/p_0), \tag{1}$$

where:

WP	=	water potential (J/kg),
R	=	universal gas constant [8.3143 J/(K mol)],
T	=	temperature (K),
W_{A}	=	molecular weight of water (18.016),
p/p_0	=	ratio of the relative vapor pressure of water in equilibrium with the system to the vapor pressure over a flat surface of water; $100(p/p_0)$ is the relative humidity.

We used the TCP, which acts as a wet-dry-bulb instrument that operates on the basis of the Peltier effect, to measure WP. When a current flows across the junction of a thermocouple, heat is either absorbed or liberated by the junction (Peltier effect). At 25°C (298 K), the magnitude of the Peltier effect for a chromel-constantan thermocouple is about 0.0179 joule/coulomb. The TCP works only for relative humidity greater than 94%, but with an accuracy of 0.1%. For relative humidity less than 94%, a large amount of current is needed to lower the temperature so the moisture in the air can be condensed at the sensing junction. This makes use of the TCP impractical. Thus, for drier conditions, we used a sensor that measures the capacitance change due to the change in relative humidity. The operational range of the capacitance sensor is from 0 to 100% relative humidity, but with an accuracy of only 2% and only at temperatures up to 160°C (320°F).

The TCPs are traditionally used for agricultural applications such as on leaves and in soil. As far as we know, this is the first time that TCPs have been used at temperatures above 40°C (104°F) and in a hard-rock environment.

Calibration of Thermocouple Psychrometer

A psychrometer has two thermocouple junctions. The copper-constantan junction serves as the reference temperature junction, and the constantan-chromel junction is the sensing junction. Current passes through the thermocouple and cools the sensing junction by the Peltier effect for a predetermined duration (cooling time). When the temperature of the junction is below the dew point, water from the air condenses on the junction. Then the Peltier current is discontinued, and the thermocouple output is recorded as the temperature of the thermocouple returns to ambient. The temperature changes rapidly toward the ambient temperature until it reaches the wet-bulb depression temperature. At this point, evaporation of the water from the junction produces a cooling effect that offsets the heat absorbed from the ambient surroundings. This cooling continues until the water is depleted and the thermocouple temperature returns to the ambient temperature (Briscoe, 1984). Three parameters are measured from a psychrometer: the reference temperature, the offset, and a series of TCP outputs. The reference temperature is the temperature at the reference junction. The offset is the microvolt difference between reference and sensing junctions before cooling. The magnitude of the offset is an indication of the temperature gradient near the TCP. The TCP output is a series of voltages as a function of time, which reflects the temperature condition during the evaporation. The datalogger starts to take data roughly at the wet-bulb depression temperature.

Laboratory calibration of the TCPs using solutions of known osmolality under controlled conditions is indispensable. The osmotic coefficient (ø) is defined (Lang, 1967) as:

$$\text{ø} = -1000\ln(p/p_0)/(nmW_A), \qquad (2)$$

where n is the number of ions per molecule of salt, and m is the moles of solute per 1000 g of solvent. Thus:

$$\text{WP} = -nmRT\text{ø}. \qquad (3)$$

Since osmolality (Ω) relates to ø by:

$$\Omega = nm\text{ø}, \qquad (4)$$

we have water potential directly related to osmolality as:

$$\text{WP} = -RT\Omega. \qquad (5)$$

The calibration procedures followed those described by Brown and Bartos (1982). The laboratory calibration setup consisted of a temperature-controllable water bath, sealed test tubes containing known concentrations of NaCl solution and stainless-steel screen-caged TCPs, a datalogger with psychrometer interface, and a personal computer to store data. Although the psychrometers used were not designed for high-temperature measurements, we found that they could take temperatures up to about 90°C (194°F). At that temperature, the cable of the TCP softened and deformed, even though the instrument was still functional. We decided to calibrate the TCPs at temperatures ranging from room temperature to 80°C (176°F) for a solution osmolality between 100 and 1000 mmol/kg, corresponding to a relative humidity range of 98.2 to 99.8%. A change in relative humidity of 1% is equivalent to a WP change of about 1.4 MPa, or 14 bars.

An aluminum block drilled with test-tube-size holes was placed inside the water bath to act as a heat sink and to prevent the circulating water from causing temperature fluctuation through direct contact with the test tubes. The test tube half-filled with NaCl solution was placed inside the hole of the aluminum block. The entire TCP sensor was submerged in the solution and sealed with silicon rubber at the top of the test tube with a 0.03-in. I.D. vent tube. The screen cage of the TCP kept the solution out, provided the solution pressure was no larger than the air pressure inside the cage. The vent tubing was normally closed except during temperature change. Approximately 2 m of each TCP cable was bundled together and submerged in the water bath to maintain the same temperature as the TCPs. Fourteen TCPs were calibrated simultaneously. All TCPs were connected to the datalogger input, and the computer was connected to the datalogger through an RS232 port. The cooling current was 8 mA, and the cooling time was 15 s. We took 29 wet-bulb readings for each channel with no wait time between readings. The measurement was repeated every 30 minutes. Appendix A describes the psychrometer datalogger program listing used for the calibration. The listing contains all of the parameters used and provides the necessary information to repeat the experiments. The psychrometer data-acquisition program for the field test was a modified version (changed to 11 channels instead of 14 channels) with the same parameters.

The calibration was carried out for six temperatures—room temperature, 40, 50, 60, 70, and 80°C (104, 122, 140, 158, and 176°F)—and for five NaCl solutions of osmolalities 100, 290, 500, 750, and 1000 mmol/kg at each temperature. We started the calibration sequence using the solution of the lowest osmolality and changed to progressively higher concentrations. This approach minimized the effect of possible solution contamination if the screen cage was not thoroughly cleaned after each solution. The following outlines the calibration procedure.

Step 1. Started at room temperature and NaCl solution of 100 mmol/kg osmolality, continuously taking data for 2 hours or until both temperature and vapor equilibria were reached.
Step 2. Changed the temperature setting to 40°C (104°F) and kept the vent tubing open until the set temperature was reached.
Step 3. Took data for 3 hours or until both temperature and vapor equilibria were achieved.
Step 4. Repeated steps 2 and 3 for temperature settings of 50, 60, 70, and 80°C (122, 140, 158, and 176°F). Turned off the heater and opened the vent tubing, taking data overnight.
Step 5. Removed the TCP from the test tube. Rinsed and cleaned the sensors with distilled water and compressed air. Removed the screen cage from the TCP and boiled the cage in distilled water for 1 minute. Restored the screen cage after it was rinsed clean and dried.
Step 6. Changed to a higher osmolality solution and repeated steps 1 to 5 until all temperatures and solutions were covered.

All calibrations were made under thermal and vapor equilibrium conditions. Thermal equilibrium was indicated when the offset was near zero. Vapor equilibrium was reached when the TCP output reached a steady state. A typical set of calibration results is shown in Fig. 1, where voltage output from a TCP with different solutions at the same temperature [40°C (104°F) in this case] is plotted at intervals of about 60 ms.

Each curve in Fig. 1 represents a complete process of evaporation. We needed to choose one data point from each curve to represent the whole process. After extensive analysis of calibration data, we found that the first data point of each series could be used to represent the measurement of a particular curve. Table 1 summarizes the calibration results of all TCPs. Each number is an average of data from all calibrated TCPs for a given temperature and solution. In Table 1, column 3 shows the average values of the offset ranging from 0.04 to –3.5 μV. Most of the mean offsets are negative, implying that the bottom of the NaCl solution in the test tube was slightly warmer (0.06°C or 0.1°F) than the top. Column 4 lists the mean outputs of the first data points, and column 6 lists their corresponding standard deviations. The mean WPs, shown in column 5, are calculated from the solution osmolalities and temperatures according to Eq. 5. The magnitudes of TCP output and WP increase with both temperature and solution osmolality. Figure 2 shows the effect of temperature on TCP output for different solutions. Figure 3 shows the effect of solution osmolality on TCP output for different temperatures. Not all TCPs survived the calibration process. Of the fourteen calibrated, four TCPs were damaged mainly by cleaning.

Lang (1967) calculated the WPs of NaCl solutions from 0 to 40°C (32 to 104°F). Brown and Bartos (1982) proposed a calibration model for the TCP over this temperature range based on their calibration results. The model assumes that the WP of the NaCl solution can be determined from cooling time, temperature, TCP output, and TCP offset.

A correction coefficient must be determined when applied to calibration data for other TCPs because different approaches may be used to represent the data from different calibrations. We extrapolated the model to higher temperatures by removing the temperature limit of 40°C (104°F), but we kept the calculated results the same as before for temperature below 40°C. We found that the WP calculated from Eq. 5 was not a simple constant ratio to that calculated from the model (WP_C), as proposed by Brown and Bartos (1982), but was a function of both temperature (t in °C) and WP_C. The regression fit from our data and the modified Brown and Bartos model was:

$$WP = 1.76 - 0.037t + 0.824WP_C + 0.007tWP_C. \tag{6}$$

Figure 4 is a scatter plot of WPs calculated from Eqs. 5 and 6 for all calibration data. The agreement is very good for the entire range of WPs and temperatures.

Clarke and Glew (1985) compiled and interpolated osmotic coefficients for NaCl solution for molalities from 0 to saturation and temperatures from 0 to 110°C (32 to 230°F). Using their data and Eq. 3, we can calculate the WP of NaCl solutions over a much larger range of molality and temperature than before.

Table 1. Summary of the TCP calibration results.

Solution osmolality (mmol/kg)	Temperature (°C)	Offset (μV)	Output (μV)	Solution WP (bar)	Output std. dev. (μV)
100	25.20	0.07	1.78	–2.47	0.30
	39.91	–1.30	1.58	–2.60	0.23
	49.83	–1.74	1.63	–2.68	0.29
	59.81	–1.96	1.76	–2.76	0.34
	70.00			–2.85	
	79.67	–2.26	2.11	–2.93	0.51
290	21.28	0.22	3.66	–7.09	0.35
	39.89	–1.91	4.47	–7.54	0.23
	50.00			–7.78	
	59.80	–1.62	6.03	–8.02	0.32
	69.95	–0.94	6.63	–8.26	0.47
	79.80	–1.15	6.88	–8.50	1.17
500	21.06	0.00	5.62	–12.22	0.40
	40.19	–1.87	7.73	–13.01	0.10
	50.21	–2.03	9.13	–13.43	0.09
	60.10	–2.32	10.43	–13.84	0.13
	70.31	–2.55	11.97	–14.27	0.26
	80.78	–2.91	13.64	–14.70	0.32
750	20.71	0.04	7.70	–18.31	0.64
	39.89	–1.48	11.22	–19.51	0.65
	49.94	–2.05	13.10	–20.13	0.72
	59.82	–2.43	15.22	–20.75	0.59
	70.18	–2.79	17.29	–21.40	0.82
	80.78	–3.27	19.06	–22.06	1.10
1000	20.18	–0.04	10.50	–24.37	0.53
	39.89	–1.62	15.89	–26.01	0.43
	49.83	–2.15	17.95	–26.84	1.30
	59.94	–2.59	20.68	–27.68	1.51
	70.21	–3.10	23.64	–28.53	1.35
	81.11	–3.50	26.53	–29.44	1.75

Field Setup

The Prototype Engineered Barrier System Field Tests (PEBSFT) were performed in G-Tunnel at the Nevada Test Site (NTS). These integrated tests measured several parameters as a function of location and time within a few meters of a heater emplaced in welded tuff (Ramirez et al., 1990b). The TCP was one of the instruments used in the PEBSFT.

Ten TCPs were installed in holes P1, P2, and P3 (see Fig. 5 for hole locations). Another TCP (Channel 4) was sealed inside a test tube filled with NaCl solution of osmolality 1000 mmol/kg. The test tube was placed inside a Thermos to keep the temperature constant. Channel 4 served as a reference channel to check the performance of the datalogger. All TCPs were installed near the bottom of the hole. In holes P1 and P2, three TCPs were installed in the sensor pockets of a rubber sleeve outside an inflatable packer (Fig. 6). By inflating the packer, we isolated each TCP from the hole environment but exposed it to the borehole wall. This arrangement assured local measurement and reduced any effect of nearby fracture systems on the measurements. The packer also blocked the grout from invading the measurement area. Another TCP was installed in front of the packer in P2 (Channel 11). For hole P3, three TCPs were bundled together in an aluminum housing backed by foam to prevent the grout from getting into the housing. The air space around the TCPs in hole P3 was 30 times larger in volume than that in P1 and P2.

Table 2 lists the locations of each TCP. Figure 5 shows the locations of these holes with respect to the heater hole.

A capacitance sensor was installed in the heater hole in front of the heater-hole packer. The output of the sensor was voltage, which was factory-calibrated to be linearly proportional to both temperature and relative humidity.

Table 2. Locations of thermocouple psychrometers.

Channel	Serial number	Hole	Mode[a]
1	29751	P1	HT packer
2	29763	P1	HT packer
3	29771	P1	HT packer
4	29772	Inst. room	Thermos
5	29760	P3	Foam
6	29769	P3	Foam
7	29759	P3	Foam
8	29764	P2	LT packer
9	29773	P2	LT packer
10	29768	P2	LT packer
11	29756	P2	LT packer

[a] HT is high temperature; LT is low temperature.

Field-Test Results

All TCPs were installed on July 27, 1988, and the holes were grouted on July 28, 1988. The capacitance sensor was installed on August 24, 1988. The heater was turned on at 11:28 a.m. on September 7, 1988. Data were taken every 30 minutes starting July 27, 1988. The sensing junction of Channel 11 was bad from the beginning; this channel only provided temperature data. A leak occurred in the pressure system outside the hole on October 12, 1988 (35th day the heater was on). Both packers were deflated and inflated again after the leak was fixed. Channels 1, 2 and 8 went bad at that time. All channels in holes P1 and P2 were affected by the leak, as indicated by glitches in the output. On November 28, 1988 (82nd day), the low-temperature packer failed at about 80°C (176°F). On January 13, 1989 (128th day), the heater power was ramped down. On May 15, 1989 (250th day), the heater was removed from the hole, and the capacitance sensor measurements were terminated.

The data plotted in Figs. 7 through 11 are from 8:33 a.m., September 7, 1988, to 8:33 a.m., July 4, 1989. The *x* axis is in days since the heater was turned on. These figures are composite plots of TCP data after smoothing by a 10-point moving window. The short dashed lines are data from hole P1, the long dashed lines are data from P2, and the solid lines are data from P3. The dotted line represents data from the reference channel.

The temperature increased with time monotonically (Fig. 7). The highest temperature measured by TCPs was about 84°C (183°F) in hole P2. The magnitude of the offset increased with temperature; the heater test data indicated that the field condition was never isothermal for the first 200 days. Offset data shown in Fig. 8 can be grouped by holes. Data from P1 have large negative offsets, and data from P2 have large positive offsets. Data from P3 have small positive offsets. A negative 60-μV offset indicates the sensing junction is 1°C (1.8°F) warmer than the reference junction, and a positive 60-μV offset indicates the sensing junction is 1°C colder (Brown and Bartos, 1982). All TCPs were installed with the sensing junction toward the bottom of the hole and the reference junction a few millimeters behind it. The TCPs in hole P1 were located with the sensing junctions toward the heater hole (see Fig. 5). Therefore, the sensing junctions of the psychrometers were warmer than the reference junctions, and consequently, negative offset values were measured. The psychrometers in holes P2 and P3 were on the other side of the heater hole; consequently, positive offset values were measured. Furthermore, the TCPs in P3 were in the bottom of a hole without a packer. Thus, the temperature in the open space had smaller gradients than those inside the rock and produced smaller offset.

The measured offsets were consistent with the locations of the TCPs relative to the heater (Fig. 8). The effects of the temperature gradients on the calculated WP were corrected using the Brown and Bartos model and Eq. (6). Figure 9 shows the TCP microvolt output; Figs. 10 and 11 show the calculated relative humidity and water potential. The initial relative humidity was about 99.5% corresponding to a WP of –5 bar. This corresponded to 15.4 g/m^3 of water in the air near the borehole wall, which was much wetter than we expected. Two broad peaks of the calculated WP stand out at about days 140 and 175. The first peak was about –65 bar in hole P3, which was below the heater and to the right. The second peak was about –45 bar in hole P2, which was above the heater and to the right. These data represent a drying and re-wetting cycle with a time difference of 35 days between the two holes.

The TCPs in hole P2 were near NE6 at distances from the collar of 5.86 and 6.16 m, and those in P3 were near NE2A at a distance from the opening of 5.89 m (see Fig. 5). Figure 12 shows the change in moisture content as a function of time, determined from the neutron measurements at these locations. Neutron data at locations below the heater (solid triangle) showed that the rock started drying out earlier than those above the heater (open square and diamond). The data from the hole below the heater became flat between days 150 and 175. It is conceivable that the rocks below the heater re-wetted within this period, but the rocks above the heater re-wetted at about day 175.

The neutron data showed a similar pattern to that from the TCPs. However, neutron data were measured every 3 to 4 weeks. Consequently, they did not have the same time resolution as the TCP data, which were measured every 30 minutes. These observed features could be explained by the gravity effect as described for neutron measurements at other locations (Ramirez and Carlson, 1990). Accordingly, as temperatures increased, the evaporation rate of pore water would increase. In unfractured rock, the gas-phase flow would be primarily outward. Water condensed above the heater would drain back to keep the boiling region wet, while water condensed below the heater would drain away from the boiling region. Thus, the rock below the heater would start drying earlier. This conceptual model also would explain why the drying peak for data above the heater is smaller than for those below the heater as indicated by the TCP data.

Figures 13 and 14 plot the temperature and relative humidity from the capacitance sensor in the heater hole. The temperature increases monotonically to about 80°C (176°F), and the relative humidity decreases slowly to about 70% during the heating phase. Both parameters return to ambient conditions monotonically after the heater is turned off.

Summary and Conclusions

The TCP experience from the PEBSFT in G-Tunnel at NTS was the first attempt to use TCPs in such a hostile environment. Because the primary goal of the TCP experiment was to determine whether the combination of laboratory calibration and field use of the TCP can provide useful data, we selected only three holes for the test. Consequently, we cannot tell the entire story of the heater test on the basis of TCP data alone. Yet, results from the TCP measurement provide information about the initial moisture condition and support some features shown by neutron measurements. This kind of consistent but redundant evidence makes the measurements of PEBSFT more credible.

In summary, we note the following:

1. The TCPs were successfully calibrated in the laboratory to measure water potential to 80°C (176°F).
2. A packer sleeve arrangement for field deployment of the TCPs was developed.
3. The initial condition in the rock from TCP measurement was about 99.5% relative humidity, which is a WP of –5 bar. This corresponded to 15.4 g/m^3 of water in the air near the borehole wall, which is much wetter than we expected.

4. Two broad drying peaks found at days 140 and 175 in hole P3 (below the heater) and P2 (above the heater) were qualitatively consistent with neutron data nearby. These features demonstrated that gravity effects on moisture movement during the heater test were very important.
5. Large offsets found in most TCPs were caused by small temperature gradients. The sign of the offset can be explained by the location of the TCPs relative to the heater. The effect of offset on the calculated WP can be corrected.
6. Temperature measurements from the TCPs supplemented the overall temperature measurement of the test.

From these results, we conclude that the TCP is a very useful instrument for monitoring the change of moisture condition in the field. It can measure minute changes, within the operation limits, that no other known instrument can. However, because of the high sensitivity of the TCP to many environmental changes, proper field installation is extremely important. Additional investigation is needed to optimize the installation procedure.

Recommendations for Future Work

Future work should emphasize a means to eliminate or control the non-isothermal effects on measurements. The long-term drift of the TCPs and the possible effects of TCP sensor-tip contamination during the test should also be investigated.

The following are our specific recommendations:

1. Change the cleaning procedure by not removing the screen cage to increase the survival rate of the TCPs during calibration.
2. Use the TCPs with Teflon-insulated cable for high-temperature measurements.
3. Use two TCPs, placed in opposite directions, for each location. In the presence of a temperature gradient, use the mean value.
4. Use crushed tuff to fill the air space around the TCP to reduce nearby air movement.
5. Use a pressure line for each packer, and use the appropriate type of packer (low- or high-temperature packer) for the location.
6. Perform post-test calibration of the TCPs to study the long-term effects, such as drift and the chemical contamination of the sensing junctions.

Acknowledgments

We thank Ralph Briscoe of Wescor and Ray Brown of the Forest Service, U.S. Department of Agriculture, for many suggestions and discussions during this research. We also thank Bill Daily, Ken Lee, and Paul Kasameyer for reviewing the manuscript and giving helpful comments. This report was prepared by the Yucca Mountain Site Characterization Project (YMP) participants as part of the Civilian Radioactive Waste Management Program. The Yucca Mountain Site Characterization Project is managed by the Yucca Mountain Site Characterization Project Office of the U.S. Department of Energy, Las Vegas, Nevada

References

Briscoe, R. D. (1984), "Thermocouple Psychrometers for Water Potential Measurements," *Proceedings, NATO Advance Study Institute on Agricultural Instrumentation*, Il Cicco (Pisa, Italy, May 27–June 9), pp. 1–14. NNA.891212.0024

Brown, R. W., and D. L. Bartos (1982), *A Calibration Model for Screen-caged Peltier Thermocouple Psychrometers*, U.S. Department of Agriculture, Washington, D.C., Forest Service Research Paper INT-293. NNA.891221.0013

Clarke, E. C. W., and D. N. Glew (1985), "Evaluation of the Thermodynamic Functions for Aqueous Sodium Chloride from Equilibrium and Calorimetric Measurements below 154°C," *J. Phys. Chem. Ref. Data* **14**(2), 489–610. NNA.910410.0170

Lang, A. R. G. (1967), "Osmotic Coefficients and Water Potentials of Sodium Chloride Solutions from 0 to 40°C," *Aust. J. Chem.* **20**, 2017–2023. NNA.891109.0068

Ramirez, A. L., and R. C. Carlson (1990), *In Situ Changes in the Moisture Content of Heated Welded Tuff Based on Thermal Neutron Measurement*, Lawrence Livermore National Laboratory, Livermore, CA, UCRL-ID-104715. (Readily available)

Ramirez, A. L., et al. (1990a), *Prototype Engineered Barrier System Field Test (PEBSFT) Progress Report Through November 1, 1988*, Lawrence Livermore National Laboratory, Livermore, CA, UCID-21640. NNA.910207.0024

Ramirez, A. L., et al. (1990b), *Prototype Engineered Barrier System Field Test (PEBSFT) Final Report*, Lawrence Livermore National Laboratory, Livermore, CA, UCRL-ID-106159. (Readily available)

Appendix A

Program List for TCP Calibration

Program: P14.doc
Flag Usage:
Input Channel Usage:1-14
Excitation Channel Usage:1-3
Continuous Analog Output Usage:
Control Port Usage:
Pulse Input Channel Usage:
Output Array Definitions:

* 1	Table 1 programs
01: 1800	Sec. execution interval
01: P17	Panel temperature
01: 1	IN card
02: 1	Loc :
02: P87	Beginning of loop
01: 0	Delay
02: 1	Loop count
03: P25	TCP instruction
01: 5	Number of psychrometers per interface
02: 2	Start input location destination for measurement Loc :
03: 1	Reference junction temperature location for base temperature measurement Loc :
04: 2	Option code for base temperature measurement 2-Hi channels measured wrt ground
05: 1	First measurement input card
06: 1	First measurement input channel
07: 1	First heating/cooling excitation card
08: 1	First heating/cooling excitation channel
09: –1900	Heating/cooling excitation voltage (negative mV)
10: 0	Heating duration time (0.01 s)
11: 0	Delay after heating before zero measurement (0.01 s)
12: 1500	Cooling duration time (0.01 s)

13: 0 Delay after cooling before wet-bulb measurement (0.01 s)
14: 100 Delay between wet-bulb measurements (0.01 s)
15: 29 Number of wet-bulb measurements per psychrometer

04: P25 TCP instruction
01: 5 Number of psychrometers per interface
02: 157 Start input location destination for measurement Loc :
03: 1 Reference junction temperature location for base temperature measurement Loc :
04: 2 Option code for base temperature measurement 2-Hi channels measured wrt ground
05: 1 First measurement input card
06: 6 First measurement input channel
07: 1 First heating/cooling excitation card
08: 2 First heating/cooling excitation channel
09: –1900 Heating/cooling excitation voltage (negative mV)
0: 0 Heating duration time (0.01 s)
11: 0 Delay after heating before zero measurement (0.01 s)
12: 1500 Cooling duration time (0.01 s)
13: 0 Delay after cooling before wet-bulb measurement (0.01 s)
14: 100 Delay between wet-bulb measurements (0.01 s)

15: 29 Number of wet-bulb measurements per psychrometer

05: P25 TCP instruction
01: 4 Number of psychrometers per interface
02: 312 Start input location destination for measurement Loc :
03: 1 Reference junction temperature location for base temperature measurement Loc :
04: 2 Option code for base temperature measurement 2-Hi channels measured wrt ground
05: 1 First measurement input card
06: 11 First measurement input channel
07: 1 First heating/cooling excitation card
08: 3 First heating/cooling excitation channel
09: –1900 Heating/cooling excitation voltage (negative mV)
10: 0 Heating duration time (0.01 s)
11: 0 Delay after heating before zero measurement (0.01 s)
12: 1500 Cooling duration time (0.01 s)
13: 0 Delay after cooling before wet-bulb measurement (0.01 s)

14: 100	Delay between wet-bulb measurements (0.01 s)
15: 29	Number of wet-bulb measurements per psychrometer
06: P86	Do
01: 10	Set flag 0 (output)
07: P80	Year
08: P77	Real time
01: 110	Day, hour-minute
09: P70	Sample 1st TCP
01: 31	Reps
02: 2	Loc
10: P86	Do
01: 10	Set flag 0 (output)
11: P80	Year
12: P77	Real time
01: 110	Day, hour-minute
13: P70	Sample 2nd TCP
01: 31	Reps
02: 33	Loc
14: P86	Do
01: 10	Set flag 0 (output)
15: P80	Year
16: P77	Real time
01: 110	Day, hour-minute
17: P70	Sample 3rd TCP
01: 31	Reps
02: 64	Loc
18: P86	Do

01: 10	Set flag 0 (output)
19: P80	Year
20: P77	Real time
01: 110	Day, hour-minute
21: P70	Sample 4th TCP
01: 31	Reps
02: 95	Loc
22: P86	Do
01: 10	Set flag 0 (output)
23: P80	Year
24: P77	Real time
01: 110	Day, hour-minute
25: P70	Sample 5th TCP
01: 31	Reps
02: 126	Loc
26: P86	Do
01: 10	Set flag 0 (output)
27: P80	Year
28: P77	Real time
01: 110	Day, hour-minute
29: P70	Sample 6th TCP
01: 31	Reps
02: 157	Loc
30: P86	Do
01: 10	Set flag 0 (output)
31: P80	Year

32: P77	Real time
01: 110	Day, hour-minute
33: P70	Sample 7th TCP
01: 31	Reps
02: 188	Loc
34: P86	Do
01: 10	Set flag 0 (output)
35: P80	Year
36: P77	Real time
01: 110	Day, hour-minute
37: P70	Sample 8th TCP
01: 31	Reps
02: 219	Loc
38: P86	Do
01: 10	Set flag 0 (output)
39: P80	Year
40: P77	Real time
01: 110	Day, hour-minute
41: P70	Sample 9th TCP
01: 31	Reps
02: 250	Loc
42: P86	Do
01: 10	Set flag 0 (output)
43: P80	Year
44: P77	Real time
01: 110	Day, hour-minute
45: P70	Sample 10th TCP

01: 31	Reps
02: 281	Loc
46: P86	Do
01: 10	Set flag 0 (output)
47: P80	Year
48: P77	Real time
01: 110	Day, hour-minute
49: P70	Sample 11th TCP
01: 31	Reps
02: 312	Loc
50: P86	Do
01: 10	Set flag 0 (output)
51: P80	Year
52: P77	Real time
01: 110	Day, hour-minute
53: P70	Sample 12th TCP
01: 31	Reps
02: 343	Loc
54: P86	Do
01: 10	Set flag 0 (output)
55: P80	Year
56: P77	Real time
01: 110	Day, hour-minute
57: P70	Sample 13th TCP
01: 31	Reps
02: 374	Loc
58: P86	Do

01: 10	Set flag 0 (output)
59: P80	Year
60: P77	Real time
01: 110	Day, hour-minute
61: P70	Sample 14th TCP
01: 31	Reps
02: 405	Loc
62: P95	End
63: P	End Table 1
* 2	Table 2 programs
01: 0	Sec. execution interval
01: P	End Table 2
* 3	Table 3 subroutines
01: P	End Table 3
* 4	Mode 4 output options
01: 1	(Tape OFF) (Printer ON)
02: 1	Printer 1200 baud
* A	Mode 10 memory allocation
01: 436	Input locations
02: 872	Intermediate locations
* C	Mode 12 security
01: 0	Security disabled
02: 0	Security code

Input Location Assignments (with comments):
(Key: T = Table Number E = Entry Number L = Location Number)
T: E: L:
1: 1: 1: Loc :

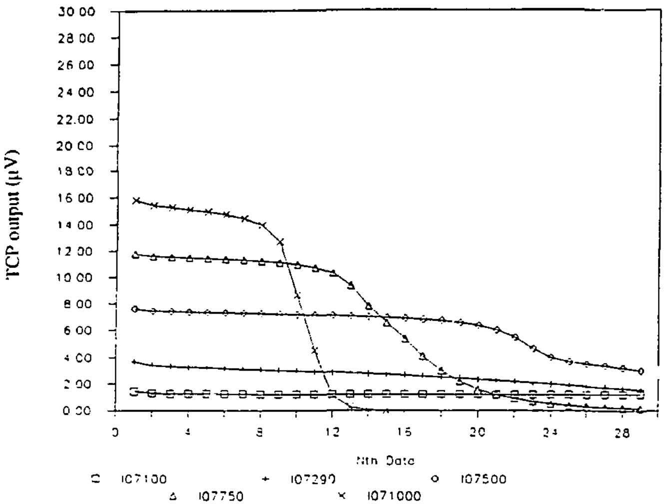

Figure 1. TCP output as a function of time for different solutions (approximately 60 ms between data points). The first three numbers of the legend for each symbol are the TCP channel number; the remaining numbers indicate the osmolality of the NaCl solution in mmol/kg.

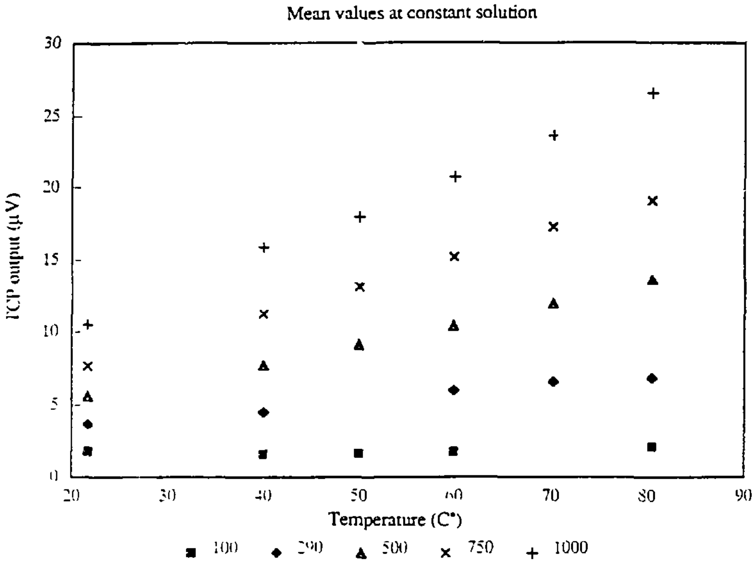

Figure 2. TCP output as a function of temperature at different solutions. The symbol legends are osmolality in mmol/ kg.

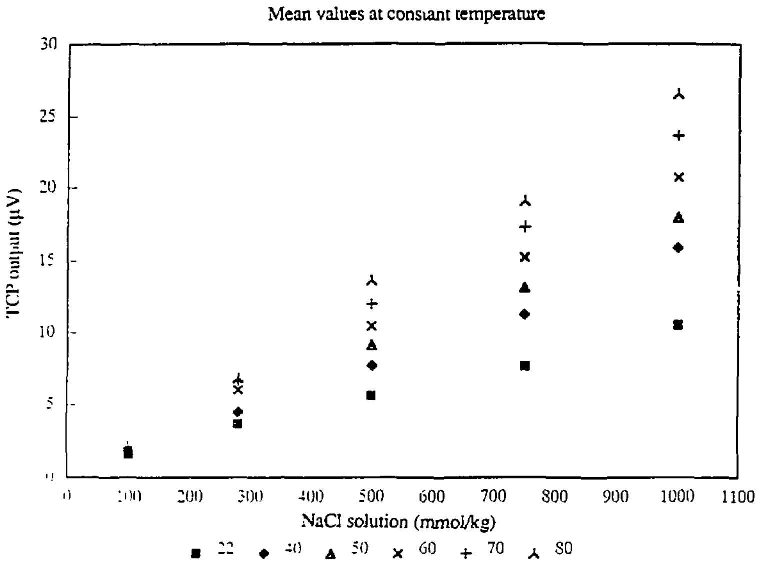

Figure 3. TCP output as a function of solution strength at different temperatures. The symbol legends are in °C.

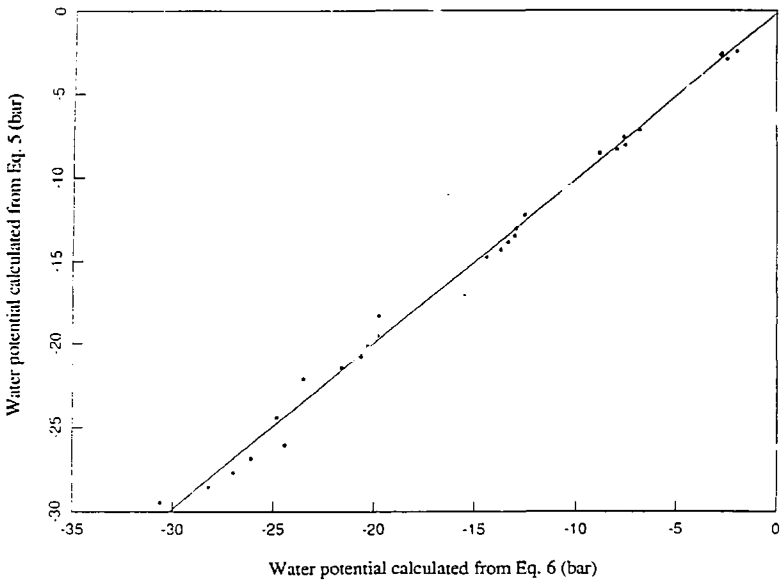

Figure 4. Scatter plot of water potentials calculated from Eqs. 5 and 6 for the laboratory TCP calibration data.

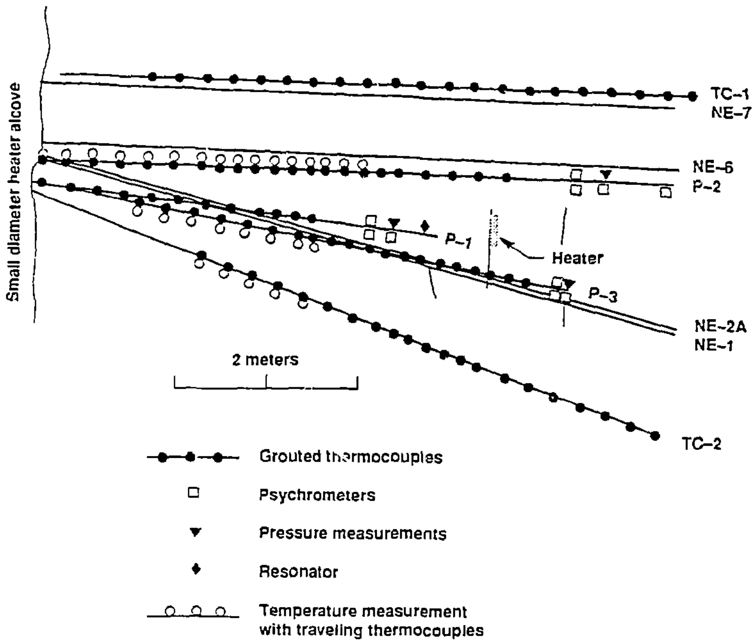

Figure 5. Side view of the as-built borehole layout as observed from the Rock Mechanics Incline (collar of the heater hole). Also shown are the locations of various sensors grouted in various boreholes. Solid circles are thermocouples for temperature measurement. Open circles are removable thermocouples for temperature measurement. Inverted solid triangles are pressure transducers mounted in the housing of the packer. Solid diamond is the resonator, a new sensor to measure moisture. (For detailed discussions of these instruments, see Ramirez et al., 1990a.)

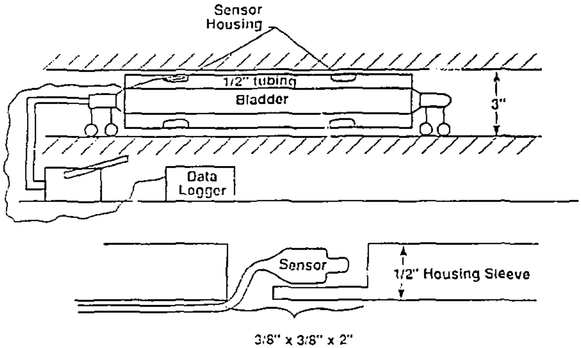

Figure 6. Packer sleeve assembly for the TCP.

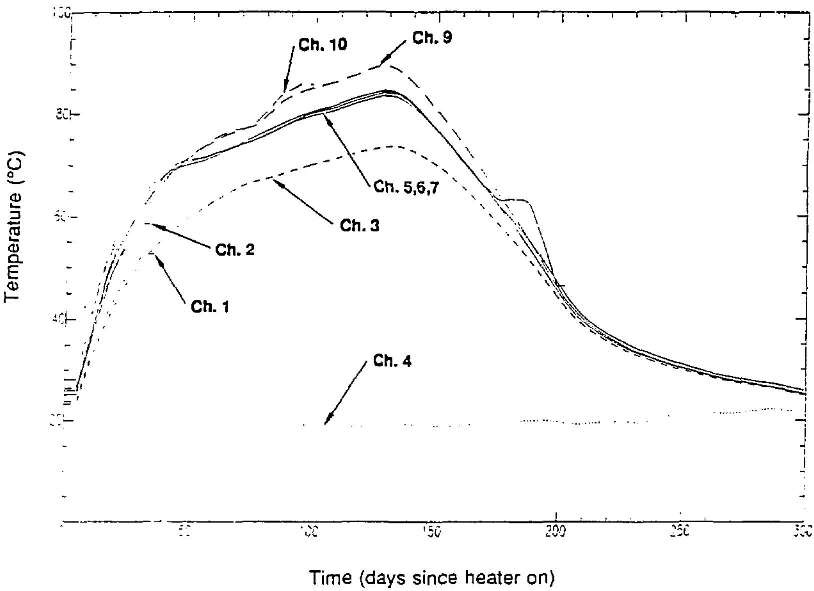

Figure 7. Temperature as a function of time for all TCPs of the heater test in G-Tunnel at NTS. Short dashed lines are data from hole P1; long dashed lines are data from P2; solid lines are data from P3; and the dotted line is for the reference channel.

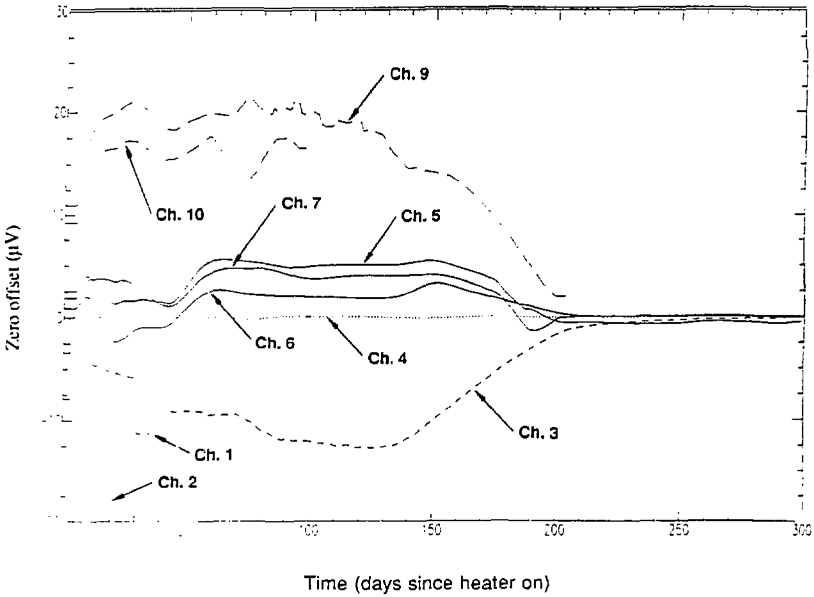

Figure 8. TCP offset as a function of time for all TCPs of the heater test in G-Tunnel at NTS. See caption of Fig. 7 for the legend.

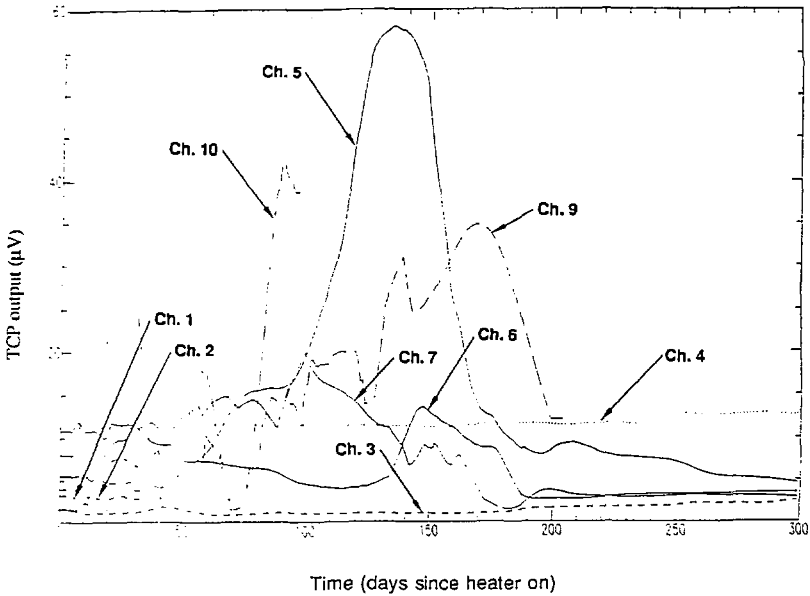

Figure 9. TCF microvoltage output as a function of time for all TCPs of the heater test in G-Tunnel at NTS. See caption of Fig. 7 for the legend.

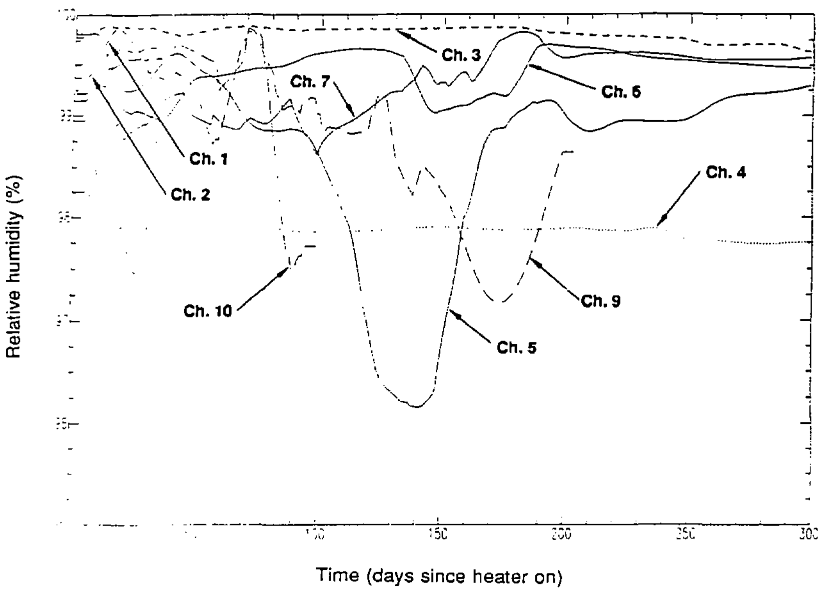

Figure 10. Calculated relative humidity as a function of time for all TCPs of the heater test in G-Tunnel at NTS. See caption of Fig. 7 for the legend.

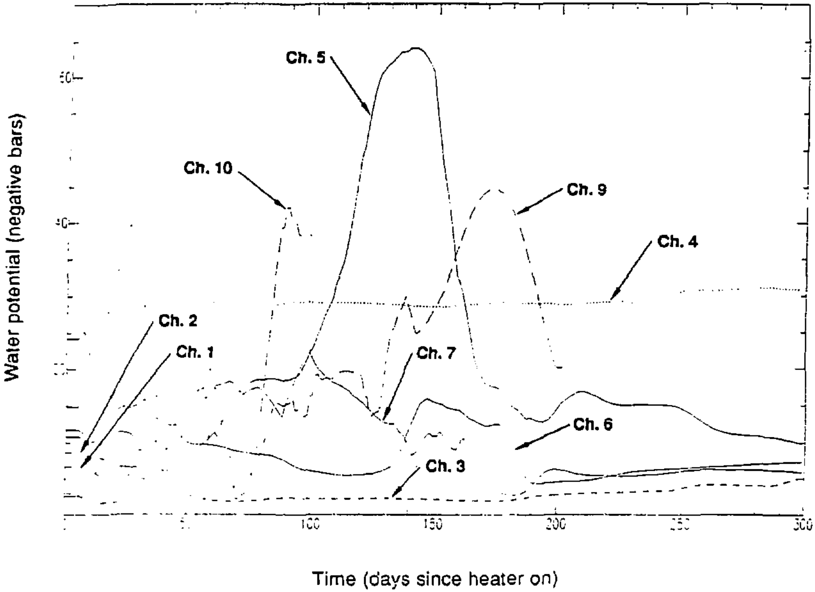

Figure 11. Calcul. .ed water potential as a function of time for all TCPs of the heater test in G-Tunnel at NTS. See caption of Fig. 7 for the legend.

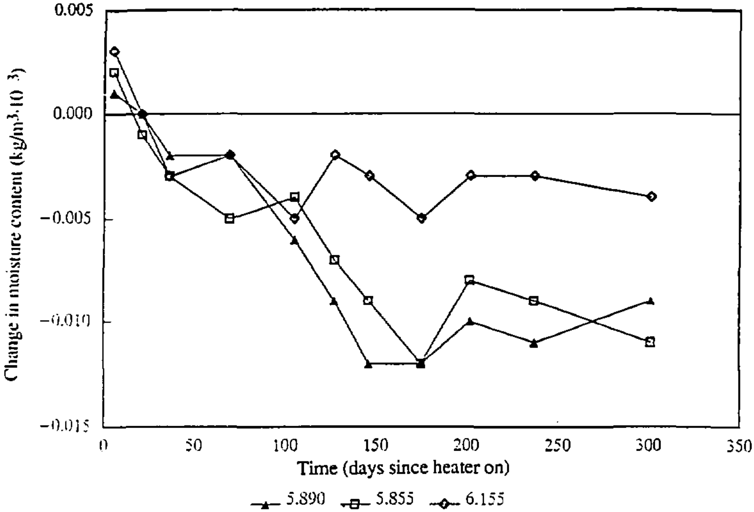

Figure 12. Change of moisture as a function of time for locations near the TCPs as determined from thermal neutron measurements.

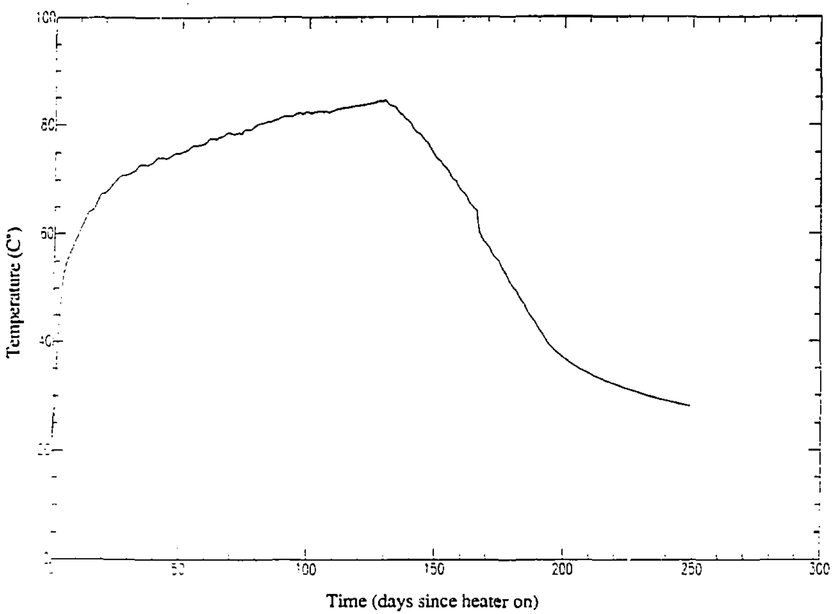

Figure 13. Measured temperature from capacitance sensor in the heater hole.

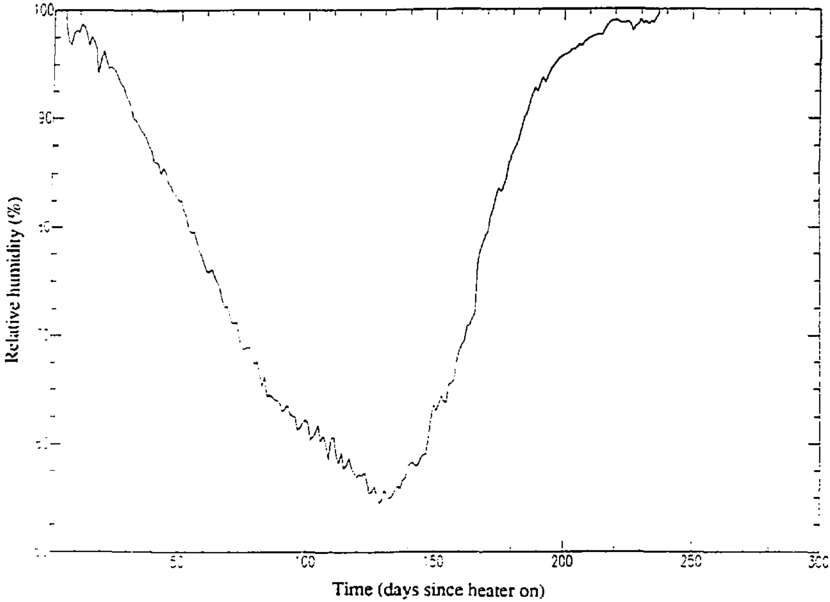

Figure 14. Measured relative humidity from capacitance sensor in the heater hole.